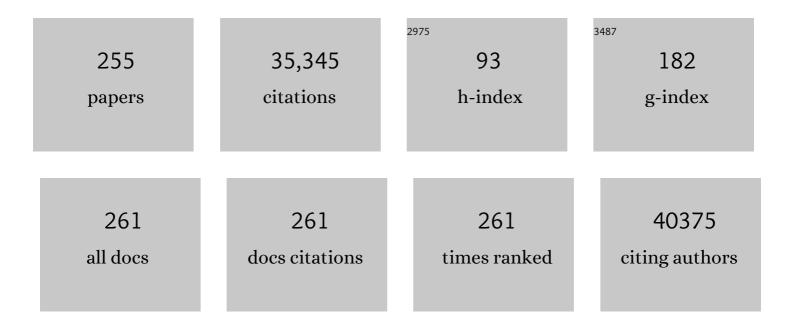
List of Publications by Year in descending order

Source: https://exaly.com/author-pdf/8966848/publications.pdf

Version: 2024-02-01



DENC CHEN

| # | Article | IF | CITATIONS |
|----|--|------|-----------|
| 1 | Tumor microenvironment-activated theranostic nanoreactor for NIR-II Photoacoustic imaging-guided tumor-specific photothermal therapy. Fundamental Research, 2024, 4, 178-187. | 3.3 | 5 |
| 2 | Promoted intramolecular photoinduced-electron transfer for multi-mode imaging-guided cancer photothermal therapy. Rare Metals, 2022, 41, 56-66. | 7.1 | 29 |
| 3 | Transdermal Photothermal-Pharmacotherapy to Remodel Adipose Tissue for Obesity and Metabolic Disorders. ACS Nano, 2022, 16, 1813-1825. | 14.6 | 32 |
| 4 | Synergistically Boosting Sodium-Storage Performance of Na ₃ V ₂ (PO ₄) ₃ by Regulating Na Sites and Constructing 3D Interconnected Carbon Nanosheet Frameworks. ACS Applied Energy Materials, 2022, 5, 2542-2552. | 5.1 | 10 |
| 5 | Template-Sacrificing Synthesis of Well-Defined Asymmetrically Coordinated Single-Atom Catalysts for Highly Efficient CO ₂ Electrocatalytic Reduction. ACS Nano, 2022, 16, 2110-2119. | 14.6 | 82 |
| 6 | Schiff base tetranuclear Zn ₂ Ln ₂ single-molecule magnets bridged by hydroxamic acid in association with near-infrared luminescence. Dalton Transactions, 2022, 51, 6918-6926. | 3.3 | 8 |
| 7 | One Stone for Multiple Birds: A Versatile Cross-Linked Poly(dimethyl siloxane) Binder Boosts Cycling Life and Rate Capability of an NCM 523 Cathode at 4.6 V. ACS Applied Materials & Interfaces, 2022, 14, 16245-16257. | 8.0 | 10 |
| 8 | POD Nanozyme optimized by charge separation engineering for light/pH activated bacteria catalytic/photodynamic therapy. Signal Transduction and Targeted Therapy, 2022, 7, 86. | 17.1 | 59 |
| 9 | Colorimetric microneedle patches for multiplexed transdermal detection of metabolites. Biosensors and Bioelectronics, 2022, 212, 114412. | 10.1 | 38 |
| 10 | Bipolar silica nanochannel array for dual-mode electrochemiluminescence and electrochemical immunosensing platform. Sensors and Actuators B: Chemical, 2022, 368, 132086. | 7.8 | 47 |
| 11 | Distinctive Formation of Bifunctional ZnCoS-rGO 3D Hollow Microsphere Flowers with Excellent Energy Storage Performances. Chemistry of Materials, 2022, 34, 5896-5911. | 6.7 | 15 |
| 12 | Cryomicroneedles for transdermal cell delivery. Nature Biomedical Engineering, 2021, 5, 1008-1018. | 22.5 | 97 |
| 13 | Orbital coupling of hetero-diatomic nickel-iron site for bifunctional electrocatalysis of CO2 reduction and oxygen evolution. Nature Communications, 2021, 12, 4088. | 12.8 | 259 |
| 14 | Rational Design of Coplanar Polypyrroleâ€Based Graphene Hydrogels with Excellent Energy‣torage Performance. Small Structures, 2021, 2, 2100073. | 12.0 | 12 |
| 15 | Graphene quantum dots assisted exfoliation of atomically-thin 2D materials and as-formed 0D/2D van der Waals heterojunction for HER. Carbon, 2021, 184, 554-561. | 10.3 | 43 |
| 16 | Fe ₃ O ₄ /Ag/Bi ₂ MoO ₆ Photoactivatable Nanozyme for Selfâ€Replenishing and Sustainable Cascaded Nanocatalytic Cancer Therapy. Advanced Materials, 2021, 33, e2106996. | 21.0 | 134 |
| 17 | Thorn-like nanostructured NiCo2S4 arrays anchoring graphite paper as self-supported electrodes for ultrahigh rate flexible supercapacitors. Electrochimica Acta, 2021, 399, 139420. | 5.2 | 12 |
| 18 | Highly biocompatible graphene quantum dots: green synthesis, toxicity comparison and fluorescence imaging. Journal of Materials Science, 2020, 55, 1198-1215. | 3.7 | 50 |

| # | Article | IF | CITATIONS |
|----|--|------|-----------|
| 19 | Diketopyrrolopyrrole-Au(I) as singlet oxygen generator for enhanced tumor photodynamic and photothermal therapy. Science China Chemistry, 2020, 63, 55-64. | 8.2 | 26 |
| 20 | Comparative Cytological and Gene Expression Analysis Reveals Potential Metabolic Pathways and Target Genes Responsive to Salt Stress in Kenaf (Hibiscus cannabinus L.). Journal of Plant Growth Regulation, 2020, 39, 1245-1260. | 5.1 | 20 |
| 21 | Ion-exchange controlled surface engineering of cobalt phosphide nanowires for enhanced hydrogen evolution. Nano Energy, 2020, 78, 105347. | 16.0 | 38 |
| 22 | Enhancing electrochemical nitrogen reduction with Ru nanowires <i>via</i> the atomic decoration of Pt. Journal of Materials Chemistry A, 2020, 8, 25142-25147. | 10.3 | 22 |
| 23 | Reduced graphene oxide foam templated by nickel foam for organ-on-a-chip engineering of cardiac constructs. Materials Science and Engineering C, 2020, 117, 111344. | 7.3 | 14 |
| 24 | Facet-Dependent Catalytic Performance of Au Nanocrystals for Electrochemical Nitrogen Reduction. ACS Applied Materials & Interfaces, 2020, 12, 41613-41619. | 8.0 | 42 |
| 25 | Remodeling Tumor Microenvironment by Multifunctional Nanoassemblies for Enhanced Photodynamic Cancer Therapy. , 2020, 2, 1268-1286. | | 40 |
| 26 | Atomically Dispersed Cobalt Trifunctional Electrocatalysts with Tailored Coordination Environment for Flexible Rechargeable Zn–Air Battery and Selfâ€Driven Water Splitting. Advanced Energy Materials, 2020, 10, 2002896. | 19.5 | 210 |
| 27 | Engineering edge-exposed MoS2 nanoflakes anchored on the 3D cross-linked carbon frameworks for enhanced lithium storage. Functional Materials Letters, 2020, 13, 2051050. | 1.2 | 1 |
| 28 | Rare-Earth Single-Atom La–N Charge-Transfer Bridge on Carbon Nitride for Highly Efficient and Selective Photocatalytic CO ₂ Reduction. ACS Nano, 2020, 14, 15841-15852. | 14.6 | 283 |
| 29 | A Highlyâ€Efficient Type I Photosensitizer with Robust Vascularâ€Disruption Activity for Hypoxicâ€andâ€Metastatic Tumor Specific Photodynamic Therapy. Small, 2020, 16, e2001059. | 10.0 | 116 |
| 30 | Metal nanodots anchored on carbon nanotubes prepared by a facile solid-state redox strategy for superior lithium storage. Functional Materials Letters, 2020, 13, 2051039. | 1.2 | 3 |
| 31 | Graphene quantum dots as full-color and stimulus responsive fluorescence ink for information encryption. Journal of Colloid and Interface Science, 2020, 579, 307-314. | 9.4 | 63 |
| 32 | Transdermal theranostics. View, 2020, 1, e21. | 5.3 | 17 |
| 33 | Transition metal dichalcogenide/multi-walled carbon nanotube-based fibers as flexible electrodes for electrocatalytic hydrogen evolution. Chemical Communications, 2020, 56, 5131-5134. | 4.1 | 28 |
| 34 | Lancing Drug Reservoirs into Subcutaneous Fat to Combat Obesity and Associated Metabolic Diseases. Small, 2020, 16, 2002872. | 10.0 | 8 |
| 35 | van der Waals Heterojunction between a Bottom-Up Grown Doped Graphene Quantum Dot and Graphene for Photoelectrochemical Water Splitting. ACS Nano, 2020, 14, 1185-1195. | 14.6 | 100 |
| 36 | iTRAQ-based comparative proteomic response analysis reveals regulatory pathways and divergent protein targets associated with salt-stress tolerance in kenaf (Hibiscus cannabinus L.). Industrial Crops and Products, 2020, 153, 112566. | 5.2 | 11 |

| # | Article | IF | CITATIONS |
|----|---|------|-----------|
| 37 | Antimicrobial Microneedle Patch for Treating Deep Cutaneous Fungal Infection. Advanced Therapeutics, 2019, 2, 1900064. | 3.2 | 28 |
| 38 | Amphiphilic graphene quantum dots as a new class of surfactants. Carbon, 2019, 153, 127-135. | 10.3 | 55 |
| 39 | Mo ₂ Câ€Derived Polyoxometalate for NIRâ€II Photoacoustic Imagingâ€Guided Chemodynamic/Photothermal Synergistic Therapy. Angewandte Chemie - International Edition, 2019, 58, 18641-18646. | 13.8 | 281 |
| 40 | Mo 2 Câ€Derived Polyoxometalate for NIRâ€II Photoacoustic Imagingâ€Guided Chemodynamic/Photothermal Synergistic Therapy. Angewandte Chemie, 2019, 131, 18814-18819. | 2.0 | 20 |
| 41 | Photothermal-pH-hypoxia responsive multifunctional nanoplatform for cancer photo-chemo therapy with negligible skin phototoxicity. Biomaterials, 2019, 221, 119422. | 11.4 | 101 |
| 42 | Bifunctional N-CoSe ₂ /3D-MXene as Highly Efficient and Durable Cathode for Rechargeable Zn–Air Battery. , 2019, 1, 432-439. | | 90 |
| 43 | Spatially Controlled Reduction and Growth of Silver in Hollow Gold Nanoshell Particles. Journal of Physical Chemistry C, 2019, 123, 10614-10621. | 3.1 | 9 |
| 44 | Recent Advances on Graphene Quantum Dots: From Chemistry and Physics to Applications. Advanced Materials, 2019, 31, e1808283. | 21.0 | 603 |
| 45 | Improved adhesion and performance of vertically-aligned mesoporous silica-nanochannel film on reduced graphene oxide for direct electrochemical analysis of human serum. Sensors and Actuators B: Chemical, 2019, 288, 133-140. | 7.8 | 38 |
| 46 | Double‣helled Nanostructure of SnO 2 @C Tubeâ€in‣nO 2 @C Tube Boosts Lithiumâ€ion Storage. Energy Technology, 2019, 7, 1801048. | 3.8 | 6 |
| 47 | Directional preparation of superhydrophobic magnetic CNF/PVA/MWCNT carbon aerogel. IET Nanobiotechnology, 2019, 13, 565-570. | 3.8 | 16 |
| 48 | Enzymatic Degradation of Graphene Quantum Dots by Human Peroxidases. Small, 2019, 15, e1905405. | 10.0 | 46 |
| 49 | Targeting graphene quantum dots to epidermal growth factor receptor for delivery of cisplatin and cellular imaging. Materials Science and Engineering C, 2019, 94, 247-257. | 7.3 | 58 |
| 50 | Mesoporous silica nanoparticles capped with graphene quantum dots as multifunctional drug carriers for photo-thermal and redox-responsive release. Microporous and Mesoporous Materials, 2019, 278, 130-137. | 4.4 | 42 |
| 51 | Boosting the Photocatalytic Ability of Cu ₂ 0 Nanowires for CO ₂ Conversion by MXene Quantum Dots. Advanced Functional Materials, 2019, 29, 1806500. | 14.9 | 354 |
| 52 | One-pot facile route to fabricate the precursor of sulfonated graphene/N-doped mesoporous carbons composites for supercapacitors. Journal of Materials Science, 2019, 54, 4180-4191. | 3.7 | 13 |
| 53 | Organic Nanotheranostics for Photoacoustic Imaging-Guided Phototherapy. Current Medicinal Chemistry, 2019, 26, 1389-1405. | 2.4 | 24 |
| 54 | Holey nickel hydroxide nanosheets for wearable solid-state fiber-supercapacitors. Nanoscale, 2018, 10, 5442-5448. | 5.6 | 50 |

| # | Article | IF | CITATIONS |
|----|--|------|-----------|
| 55 | Organic Dye Based Nanoparticles for Cancer Phototheranostics. Small, 2018, 14, e1704247. | 10.0 | 226 |
| 56 | Recent progress in the development of near-infrared organic photothermal and photodynamic nanotherapeutics. Biomaterials Science, 2018, 6, 746-765. | 5.4 | 250 |
| 57 | Simultaneous label-free and pretreatment-free detection of heavy metal ions in complex samples using electrodes decorated with vertically ordered silica nanochannels. Sensors and Actuators B: Chemical, 2018, 259, 364-371. | 7.8 | 86 |
| 58 | Analysis of chloroplast differences in leaves of rice isonuclear alloplasmic lines. Protoplasma, 2018, 255, 863-871. | 2.1 | 15 |
| 59 | Biodegradable PLA Nonwoven Fabric with Controllable Wettability for Efficient Water Purification and Photocatalysis Degradation. ACS Sustainable Chemistry and Engineering, 2018, 6, 2445-2452. | 6.7 | 87 |
| 60 | Quasi-homogeneous carbocatalysis for one-pot selective conversion of carbohydrates to 5-hydroxymethylfurfural using sulfonated graphene quantum dots. Carbon, 2018, 136, 224-233. | 10.3 | 60 |
| 61 | Nanoplasmonic Sensing from the Human Vision Perspective. Analytical Chemistry, 2018, 90, 4916-4924. | 6.5 | 43 |
| 62 | Graphene quantum dot engineered nickel-cobalt phosphide as highly efficient bifunctional catalyst for overall water splitting. Nano Energy, 2018, 48, 284-291. | 16.0 | 143 |
| 63 | Systematic Bandgap Engineering of Graphene Quantum Dots and Applications for Photocatalytic Water Splitting and CO ₂ Reduction. ACS Nano, 2018, 12, 3523-3532. | 14.6 | 341 |
| 64 | Graphene quantum dots based fluorescence turn-on nanoprobe for highly sensitive and selective imaging of hydrogen sulfide in living cells. Biomaterials Science, 2018, 6, 779-784. | 5.4 | 42 |
| 65 | Tunable excitonic emission of monolayer WS2 for the optical detection of DNA nucleobases. Nano Research, 2018, 11, 1744-1754. | 10.4 | 20 |
| 66 | Oxygenic Hybrid Semiconducting Nanoparticles for Enhanced Photodynamic Therapy. Nano Letters, 2018, 18, 586-594. | 9.1 | 294 |
| 67 | "Wax‣ealed―Theranostic Nanoplatform for Enhanced Afterglow Imaging–Guided Photothermally Triggered Photodynamic Therapy. Advanced Functional Materials, 2018, 28, 1804317. | 14.9 | 97 |
| 68 | Self-implantable double-layered micro-drug-reservoirs for efficient and controlled ocular drug delivery. Nature Communications, 2018, 9, 4433. | 12.8 | 209 |
| 69 | Nanochannel-Confined Graphene Quantum Dots for Ultrasensitive Electrochemical Analysis of Complex Samples. ACS Nano, 2018, 12, 12673-12681. | 14.6 | 129 |
| 70 | Solution-processable 2D semiconductors for high-performance large-area electronics. Nature, 2018, 562, 254-258. | 27.8 | 644 |
| 71 | Insight into the charge transport correlation in Au _x clusters and graphene quantum dots deposited on TiO ₂ nanotubes for photoelectrochemical oxygen evolution. Journal of Materials Chemistry A, 2018, 6, 11154-11162. | 10.3 | 89 |
| 72 | Ordered Mesoporous Carbons Loading on Graphene after Different Molten Salt Activations for Supercapacitor Applications. Energy Technology, 2018, 6, 2273-2281. | 3.8 | 13 |

| # | Article | IF | CITATIONS |
|----|--|------|-----------|
| 73 | An aza-BODIPY photosensitizer for photoacoustic and photothermal imaging guided dual modal cancer phototherapy. Journal of Materials Chemistry B, 2017, 5, 1566-1573. | 5.8 | 96 |
| 74 | Functionalization of Biodegradable PLA Nonwoven Fabric as Superoleophilic and Superhydrophobic Material for Efficient Oil Absorption and Oil/Water Separation. ACS Applied Materials & Interfaces, 2017, 9, 5968-5973. | 8.0 | 241 |
| 75 | Inflection Point of the Localized Surface Plasmon Resonance Peak: A General Method to Improve the Sensitivity. ACS Sensors, 2017, 2, 235-242. | 7.8 | 52 |
| 76 | Ternary Chalcogenide Nanosheets with Ultrahigh Photothermal Conversion Efficiency for Photoacoustic Theranostics. Small, 2017, 13, 1604139. | 10.0 | 83 |
| 77 | Organic Nanoprobe Cocktails for Multilocal and Multicolor Fluorescence Imaging of Reactive Oxygen Species. Advanced Functional Materials, 2017, 27, 1700493. | 14.9 | 82 |
| 78 | An elaborate strategy for fabricating one-dimensional quasi-hollow nanostructure of tin dioxide@carbon composite with improved lithium storage performance. Carbon, 2017, 118, 634-641. | 10.3 | 22 |
| 79 | Facile and scalable preparation of highly luminescent N,S co-doped graphene quantum dots and their application for parallel detection of multiple metal ions. Journal of Materials Chemistry B, 2017, 5, 6593-6600. | 5.8 | 106 |
| 80 | Cobalt Phosphide Double-Shelled Nanocages: Broadband Light-Harvesting Nanostructures for Efficient Photothermal Therapy and Self-Powered Photoelectrochemical Biosensing. Small, 2017, 13, 1700798. | 10.0 | 60 |
| 81 | Activatable Photoacoustic Nanoprobes for In Vivo Ratiometric Imaging of Peroxynitrite. Advanced Materials, 2017, 29, 1604764. | 21.0 | 220 |
| 82 | Sonochemical fabrication of folic acid functionalized multistimuli-responsive magnetic graphene oxide-based nanocapsules for targeted drug delivery. Chemical Engineering Journal, 2017, 326, 839-848. | 12.7 | 40 |
| 83 | A Graphene Quantum Dots–Hypochlorite Hybrid System for the Quantitative Fluorescent Determination of Total Antioxidant Capacity. Small, 2017, 13, 1700709. | 10.0 | 21 |
| 84 | Spectral and spatial characterization of upconversion luminescent nanocrystals as nanowaveguides. Nanoscale, 2017, 9, 9238-9245. | 5.6 | 13 |
| 85 | pH-Triggered and Enhanced Simultaneous Photodynamic and Photothermal Therapy Guided by Photoacoustic and Photothermal Imaging. Chemistry of Materials, 2017, 29, 5216-5224. | 6.7 | 170 |
| 86 | Achievement of significantly improved lithium storage for novel clew-like Li 4 Ti 5 O 12 anode assembled by ultrafine nanowires. Journal of Power Sources, 2017, 350, 49-55. | 7.8 | 24 |
| 87 | Small-molecule diketopyrrolopyrrole-based therapeutic nanoparticles for photoacoustic imaging-guided photothermal therapy. Nano Research, 2017, 10, 794-801. | 10.4 | 50 |
| 88 | Molecular‣evel Design of Hierarchically Porous Carbons Codoped with Nitrogen and Phosphorus Capable of In Situ Selfâ€Activation for Sustainable Energy Systems. Small, 2017, 13, 1602010. | 10.0 | 47 |
| 89 | Transdermal Delivery of Antiâ€Obesity Compounds to Subcutaneous Adipose Tissue with Polymeric Microneedle Patches. Small Methods, 2017, 1, 1700269. | 8.6 | 88 |
| 90 | Diketopyrrolopyrrole-Based Photosensitizers Conjugated with Chemotherapeutic Agents for Multimodal Tumor Therapy. ACS Applied Materials & Interfaces, 2017, 9, 30398-30405. | 8.0 | 39 |

| # | Article | IF | CITATIONS |
|-----|---|------|-----------|
| 91 | Regulating Near-Infrared Photodynamic Properties of Semiconducting Polymer Nanotheranostics for Optimized Cancer Therapy. ACS Nano, 2017, 11, 8998-9009. | 14.6 | 239 |
| 92 | Angiotensin type 2 receptor activation promotes browning of white adipose tissue and brown adipogenesis. Signal Transduction and Targeted Therapy, 2017, 2, 17022. | 17.1 | 47 |
| 93 | A Swellable Microneedle Patch to Rapidly Extract Skin Interstitial Fluid for Timely Metabolic Analysis. Advanced Materials, 2017, 29, 1702243. | 21.0 | 303 |
| 94 | The synergistic effect supported Li 4 Ti 5 O 12 anode with advanced lithium storage performance. Materials Chemistry and Physics, 2017, 201, 362-371. | 4.0 | 2 |
| 95 | Sweet graphene quantum dots for imaging carbohydrate receptors in live cells. FlatChem, 2017, 5, 25-32. | 5.6 | 46 |
| 96 | Integrative analyses of translatome and transcriptome reveal important translational controls in brown and white adipose regulated by microRNAs. Scientific Reports, 2017, 7, 5681. | 3.3 | 10 |
| 97 | Surface Modified Ti ₃ C ₂ MXene Nanosheets for Tumor Targeting Photothermal/Photodynamic/Chemo Synergistic Therapy. ACS Applied Materials & Interfaces, 2017, 9, 40077-40086. | 8.0 | 491 |
| 98 | Ultralong Phosphorescence of Waterâ€6oluble Organic Nanoparticles for In Vivo Afterglow Imaging. Advanced Materials, 2017, 29, 1606665. | 21.0 | 419 |
| 99 | Thiophene-derived polymer dots for imaging endocytic compartments in live cells and broad-spectrum bacterial killing. Materials Chemistry Frontiers, 2017, 1, 152-157. | 5.9 | 11 |
| 100 | Dynamic transcriptome changes during adipose tissue energy expenditure reveal critical roles for long noncoding RNA regulators. PLoS Biology, 2017, 15, e2002176. | 5.6 | 81 |
| 101 | Weavable, Highâ€Performance, Solid‣tate Supercapacitors Based on Hybrid Fibers Made of Sandwiched Structure of MWCNT/rGO/MWCNT. Advanced Electronic Materials, 2016, 2, 1600102. | 5.1 | 47 |
| 102 | Controlling armchair and zigzag edges in oxidative cutting of graphene. Journal of Materials Chemistry C, 2016, 4, 6539-6545. | 5.5 | 8 |
| 103 | Monitoring Dynamic Cellular Redox Homeostasis Using Fluorescence-Switchable Graphene Quantum Dots. ACS Nano, 2016, 10, 11475-11482. | 14.6 | 71 |
| 104 | Macromol. Rapid Commun. 23/2016. Macromolecular Rapid Communications, 2016, 37, 1980-1980. | 3.9 | 0 |
| 105 | Nanowires assembled from MnCo2O4@C nanoparticles for water splitting and all-solid-state supercapacitor. Nano Research, 2016, 9, 1300-1309. | 10.4 | 87 |
| 106 | Multilayered semiconducting polymer nanoparticles with enhanced NIR fluorescence for molecular imaging in cells, zebrafish and mice. Chemical Science, 2016, 7, 5118-5125. | 7.4 | 113 |
| 107 | Smartphone spectrometer for colorimetric biosensing. Analyst, The, 2016, 141, 3233-3238. | 3.5 | 125 |
| 108 | Metal–organic framework derived CoSe2 nanoparticles anchored on carbon fibers as bifunctional electrocatalysts for efficient overall water splitting. Nano Research, 2016, 9, 2234-2243. | 10.4 | 215 |

| # | Article | IF | CITATIONS |
|-----|--|------|-----------|
| 109 | Peptide Functionalized Gold Nanoparticles with Optimized Particle Size and Concentration for Colorimetric Assay Development: Detection of Cardiac Troponin I. ACS Sensors, 2016, 1, 1416-1422. | 7.8 | 79 |
| 110 | Highly Swellable, Dualâ€Responsive Hydrogels Based on PNIPAM and Redox Active Poly(ferrocenylsilane) Poly(ionic liquid)s: Synthesis, Structure, and Properties. Macromolecular Rapid Communications, 2016, 37, 1939-1944. | 3.9 | 43 |
| 111 | Achieving stable and efficient water oxidation by incorporating NiFe layered double hydroxide nanoparticles into aligned carbon nanotubes. Nanoscale Horizons, 2016, 1, 156-160. | 8.0 | 99 |
| 112 | Ultrasensitive Profiling of Metabolites Using Tyramine-Functionalized Graphene Quantum Dots. ACS Nano, 2016, 10, 3622-3629. | 14.6 | 145 |
| 113 | Detection of Matrilysin Activity Using Polypeptide Functionalized Reduced Graphene Oxide Field-Effect Transistor Sensor. Analytical Chemistry, 2016, 88, 2994-2998. | 6.5 | 45 |
| 114 | Quantum dots derived from two-dimensional materials and their applications for catalysis and energy. Chemical Society Reviews, 2016, 45, 2239-2262. | 38.1 | 391 |
| 115 | Regulatory networks of non-coding RNAs in brown/beige adipogenesis. Bioscience Reports, 2015, 35, . | 2.4 | 28 |
| 116 | A Novel Electroactive Polymer for pHâ€independent Oxygen Sensing. Electroanalysis, 2015, 27, 2745-2752. | 2.9 | 3 |
| 117 | Reporter-encapsulated liposomes on graphene field effect transistors for signal enhanced detection of physiological enzymes. Physical Chemistry Chemical Physics, 2015, 17, 3451-3456. | 2.8 | 8 |
| 118 | Graphene quantum dots functionalized gold nanoparticles for sensitive electrochemical detection of heavy metal ions. Electrochimica Acta, 2015, 172, 7-11. | 5.2 | 200 |
| 119 | Microfiber devices based on carbon materials. Materials Today, 2015, 18, 215-226. | 14.2 | 57 |
| 120 | Hybrid Fibers Made of Molybdenum Disulfide, Reduced Graphene Oxide, and Multiâ€Walled Carbon Nanotubes for Solid‣tate, Flexible, Asymmetric Supercapacitors. Angewandte Chemie - International Edition, 2015, 54, 4651-4656. | 13.8 | 334 |
| 121 | MOF-directed templating synthesis of a porous multicomponent dodecahedron with hollow interiors for enhanced lithium-ion battery anodes. Journal of Materials Chemistry A, 2015, 3, 8483-8488. | 10.3 | 178 |
| 122 | De Novo Reconstruction of Adipose Tissue Transcriptomes Reveals Long Non-coding RNA Regulators of Brown Adipocyte Development. Cell Metabolism, 2015, 21, 764-776. | 16.2 | 201 |
| 123 | Nitrogen and phosphorus co-doped graphene quantum dots: synthesis from adenosine triphosphate, optical properties, and cellular imaging. Nanoscale, 2015, 7, 8159-8165. | 5.6 | 174 |
| 124 | Apelin Enhances Brown Adipogenesis and Browning of White Adipocytes. Journal of Biological Chemistry, 2015, 290, 14679-14691. | 3.4 | 87 |
| 125 | Graphene–bacteria composite for oxygen reduction and lithium ion batteries. Journal of Materials Chemistry A, 2015, 3, 12873-12879. | 10.3 | 30 |
| 126 | Strategies for enhancing the sensitivity of plasmonic nanosensors. Nano Today, 2015, 10, 213-239. | 11.9 | 356 |

| # | Article | IF | CITATIONS |
|-----|---|------|-----------|
| 127 | Graphene quantum dots for ultrasensitive detection of acetylcholinesterase and its inhibitors. 2D Materials, 2015, 2, 034018. | 4.4 | 33 |
| 128 | A graphene quantum dot-based FRET system for nuclear-targeted and real-time monitoring of drug delivery. Nanoscale, 2015, 7, 15477-15486. | 5.6 | 83 |
| 129 | Peptide-Assembled Graphene Oxide as a Fluorescent Turn-On Sensor for Lipopolysaccharide (Endotoxin) Detection. Analytical Chemistry, 2015, 87, 9408-9412. | 6.5 | 100 |
| 130 | Glowing Graphene Quantum Dots and Carbon Dots: Properties, Syntheses, and Biological Applications. Small, 2015, 11, 1620-1636. | 10.0 | 1,770 |
| 131 | Layer-by-layer printing of laminated graphene-based interdigitated microelectrodes for flexible planar micro-supercapacitors. Electrochemistry Communications, 2015, 51, 33-36. | 4.7 | 169 |
| 132 | Three-Dimensional Porous Architectures of Carbon Nanotubes and Graphene Sheets for Energy Applications. Frontiers in Energy Research, 2014, 2, . | 2.3 | 14 |
| 133 | Optimizing the Refractive Index Sensitivity of Plasmonically Coupled Gold Nanoparticles. Plasmonics, 2014, 9, 773-780. | 3.4 | 52 |
| 134 | Facile Synthesis of Graphene Quantum Dots from 3D Graphene and their Application for Fe ³⁺ Sensing. Advanced Functional Materials, 2014, 24, 3021-3026. | 14.9 | 446 |
| 135 | Apelin Attenuates Oxidative Stress in Human Adipocytes. Journal of Biological Chemistry, 2014, 289, 3763-3774. | 3.4 | 92 |
| 136 | Free-standing electrochemical electrode based on Ni(OH) ₂ /3D graphene foam for nonenzymatic glucose detection. Nanoscale, 2014, 6, 7424-7429. | 5.6 | 174 |
| 137 | Fluorescent quantum dots derived from PEDOT and their applications in optical imaging and sensing. Materials Horizons, 2014, 1, 529-534. | 12.2 | 30 |
| 138 | Curvature of the Localized Surface Plasmon Resonance Peak. Analytical Chemistry, 2014, 86, 7399-7405. | 6.5 | 48 |
| 139 | Biofunctionalized Gold Nanoparticles for Colorimetric Sensing of Botulinum Neurotoxin A Light Chain. Analytical Chemistry, 2014, 86, 2345-2352. | 6.5 | 71 |
| 140 | Three-Dimensional Graphene-Carbon Nanotube Hybrid for High-Performance Enzymatic Biofuel Cells. ACS Applied Materials & Interfaces, 2014, 6, 3387-3393. | 8.0 | 136 |
| 141 | Fabrication of Ultralong Hybrid Microfibers from Nanosheets of Reduced Graphene Oxide and Transitionâ€Metal Dichalcogenides and their Application as Supercapacitors. Angewandte Chemie - International Edition, 2014, 53, 12576-12580. | 13.8 | 119 |
| 142 | Heteroatom-doped graphene materials: syntheses, properties and applications. Chemical Society Reviews, 2014, 43, 7067-7098. | 38.1 | 1,547 |
| 143 | Revealing the tunable photoluminescence properties of graphene quantum dots. Journal of Materials Chemistry C, 2014, 2, 6954-6960. | 5.5 | 530 |
| 144 | Fluorescence quenching between unbonded graphene quantum dots and gold nanoparticles upon simple mixing. RSC Advances, 2014, 4, 35673-35677. | 3.6 | 31 |

| # | Article | IF | CITATIONS |
|-----|---|------|-----------|
| 145 | Fourâ€Layer Tin–Carbon Nanotube Yolk–Shell Materials for Highâ€Performance Lithiumâ€Ion Batteries. ChemSusChem, 2014, 7, 1407-1414. | 6.8 | 30 |
| 146 | Solution-processed flexible transparent conductors based on carbon nanotubes and silver grid hybrid films. Nanoscale, 2014, 6, 4560-4565. | 5.6 | 22 |
| 147 | TiN@VN Nanowire Arrays on 3D Carbon for Highâ€Performance Supercapacitors. ChemElectroChem, 2014, 1, 1027-1030. | 3.4 | 22 |
| 148 | Spatiotemporal catalytic dynamics within single nanocatalysts revealed by single-molecule microscopy. Chemical Society Reviews, 2014, 43, 1107-1117. | 38.1 | 135 |
| 149 | Phase-controlled synthesis of α-NiS nanoparticles confined in carbon nanorods for High Performance Supercapacitors. Scientific Reports, 2014, 4, 7054. | 3.3 | 101 |
| 150 | 2D single- or double-layered vanadium oxide nanosheet assembled 3D microflowers: controlled synthesis, growth mechanism, and applications. Nanoscale, 2013, 5, 7790. | 5.6 | 27 |
| 151 | Solid-Phase Colorimetric Sensor Based on Gold Nanoparticle-Loaded Polymer Brushes: Lead Detection as a Case Study. Analytical Chemistry, 2013, 85, 4094-4099. | 6.5 | 84 |
| 152 | Gold nanoparticles decorated reduced graphene oxide for detecting the presence and cellular release of nitric oxide. Electrochimica Acta, 2013, 111, 441-446. | 5.2 | 69 |
| 153 | Control of Adipogenesis by the Autocrine Interplays between Angiotensin 1–7/Mas Receptor and Angiotensin II/AT1 Receptor Signaling Pathways. Journal of Biological Chemistry, 2013, 288, 15520-15531. | 3.4 | 57 |
| 154 | Gallium-Doped Tin Oxide Nano-Cuboids for Improved Dye Sensitized Solar Cell. ACS Applied Materials & Interfaces, 2013, 5, 11377-11382. | 8.0 | 33 |
| 155 | In Situ Charge-Transfer-Induced Transition from Metallic to Semiconducting Single-Walled Carbon Nanotubes. Chemistry of Materials, 2013, 25, 4464-4470. | 6.7 | 9 |
| 156 | Increase of riboflavin biosynthesis underlies enhancement of extracellular electron transfer of Shewanella in alkaline microbial fuel cells. Bioresource Technology, 2013, 130, 763-768. | 9.6 | 86 |
| 157 | Nanoporous tin oxide photoelectrode prepared by electrochemical anodization in aqueous ammonia to improve performance of dye sensitized solar cell. Journal of Renewable and Sustainable Energy, 2013, 5, 023120. | 2.0 | 21 |
| 158 | High capacitive performance of flexible and binder-free graphene–polypyrrole composite membrane based on in situ reduction of graphene oxide and self-assembly. Nanoscale, 2013, 5, 9860. | 5.6 | 93 |
| 159 | Peptide functionalized gold nanoparticles for colorimetric detection of matrilysin (MMP-7) activity. Nanoscale, 2013, 5, 8973. | 5.6 | 75 |
| 160 | Memory Devices Using a Mixture of MoS ₂ and Graphene Oxide as the Active Layer. Small, 2013, 9, 727-731. | 10.0 | 144 |
| 161 | Ferritin-Templated Synthesis and Self-Assembly of Pt Nanoparticles on a Monolithic Porous Graphene Network for Electrocatalysis in Fuel Cells. ACS Applied Materials & Interfaces, 2013, 5, 782-787. | 8.0 | 96 |
| 162 | A hierarchically structured composite of Mn ₃ O ₄ /3D graphene foam for flexible nonenzymatic biosensors. Journal of Materials Chemistry B, 2013, 1, 110-115. | 5.8 | 137 |

| # | Article | IF | CITATIONS |
|-----|---|------|-----------|
| 163 | Enzymeless multi-sugar fuel cells with high power output based on 3D graphene–Co3O4 hybrid electrodes. Physical Chemistry Chemical Physics, 2013, 15, 9170. | 2.8 | 42 |
| 164 | Non-enzymatic detection of hydrogen peroxide using a functionalized three-dimensional graphene electrode. Electrochemistry Communications, 2013, 26, 81-84. | 4.7 | 109 |
| 165 | Graphene Quantum Dots as Universal Fluorophores and Their Use in Revealing Regulated Trafficking of Insulin Receptors in Adipocytes. ACS Nano, 2013, 7, 6278-6286. | 14.6 | 229 |
| 166 | The Electrical Detection of Lead Ions Using Goldâ€Nanoparticle―and DNAzymeâ€Functionalized Graphene Device. Advanced Healthcare Materials, 2013, 2, 271-274. | 7.6 | 73 |
| 167 | Kainate Receptors Mediate Regulated Exocytosis of Secretory Phospholipase A2 in SH-SY5Y Neuroblastoma Cells. NeuroSignals, 2012, 20, 72-85. | 0.9 | 9 |
| 168 | RGD-Peptide Functionalized Graphene Biomimetic Live-Cell Sensor for Real-Time Detection of Nitric Oxide Molecules. ACS Nano, 2012, 6, 6944-6951. | 14.6 | 172 |
| 169 | Synthesis of a MnO2–graphene foam hybrid with controlled MnO2 particle shape and its use as a supercapacitor electrode. Carbon, 2012, 50, 4865-4870. | 10.3 | 214 |
| 170 | 3D Graphene Foam as a Monolithic and Macroporous Carbon Electrode for Electrochemical Sensing. ACS Applied Materials & Interfaces, 2012, 4, 3129-3133. | 8.0 | 292 |
| 171 | Hybrid structure of zinc oxide nanorods and three dimensional graphene foam for supercapacitor and electrochemical sensor applications. RSC Advances, 2012, 2, 4364. | 3.6 | 285 |
| 172 | Real-time DNA detection using Pt nanoparticle-decorated reduced graphene oxide field-effect transistors. Nanoscale, 2012, 4, 293-297. | 5.6 | 185 |
| 173 | Synthesis of graphene–carbon nanotube hybrid foam and its use as a novel three-dimensional electrode for electrochemical sensing. Journal of Materials Chemistry, 2012, 22, 17044. | 6.7 | 197 |
| 174 | 3D Graphene–Cobalt Oxide Electrode for High-Performance Supercapacitor and Enzymeless Glucose Detection. ACS Nano, 2012, 6, 3206-3213. | 14.6 | 1,510 |
| 175 | Macroporous and Monolithic Anode Based on Polyaniline Hybridized Three-Dimensional Graphene for High-Performance Microbial Fuel Cells. ACS Nano, 2012, 6, 2394-2400. | 14.6 | 520 |
| 176 | Superhydrophobic and superoleophilic hybrid foam of graphene and carbon nanotube for selective removal of oils or organic solvents from the surface of water. Chemical Communications, 2012, 48, 10660. | 4.1 | 471 |
| 177 | Macroporous foam of reduced graphene oxides prepared by lyophilization. Materials Research Bulletin, 2012, 47, 4335-4339. | 5.2 | 18 |
| 178 | Apelin inhibits adipogenesis and lipolysis through distinct molecular pathways. Molecular and Cellular Endocrinology, 2012, 362, 227-241. | 3.2 | 89 |
| 179 | Electrodeposited Pt on three-dimensional interconnected graphene as a free-standing electrode for fuel cell application. Journal of Materials Chemistry, 2012, 22, 5286. | 6.7 | 210 |
| 180 | Biological and chemical sensors based on graphene materials. Chemical Society Reviews, 2012, 41, 2283-2307. | 38.1 | 1,591 |

| # | Article | IF | CITATIONS |
|-----|---|------|-----------|
| 181 | A graphene–cobalt oxide based needle electrode for non-enzymatic glucose detection in micro-droplets. Chemical Communications, 2012, 48, 6490. | 4.1 | 155 |
| 182 | High-density metallic nanogaps fabricated on solid substrates used for surface enhanced Raman scattering. Nanoscale, 2012, 4, 860-863. | 5.6 | 43 |
| 183 | Template-free synthesis of large anisotropic gold nanostructures on reduced graphene oxide. Nanoscale, 2012, 4, 3055. | 5.6 | 28 |
| 184 | On-chip diameter-dependent conversion of metallic to semiconducting single-walled carbon nanotubes by immersion in 2-ethylanthraquinone. RSC Advances, 2012, 2, 1275-1281. | 3.6 | 5 |
| 185 | The electrical properties of graphene modified by bromophenyl groups derived from a diazonium compound. Carbon, 2012, 50, 1517-1522. | 10.3 | 45 |
| 186 | Supercapacitor electrode based on three-dimensional graphene–polyaniline hybrid. Materials Chemistry and Physics, 2012, 134, 576-580. | 4.0 | 125 |
| 187 | Apelin secretion and expression of apelin receptors in 3T3-L1 adipocytes are differentially regulated by angiotensin type 1 and type 2 receptors. Molecular and Cellular Endocrinology, 2012, 351, 296-305. | 3.2 | 21 |
| 188 | Comparative studies on single-layer reduced graphene oxide films obtained by electrochemical reduction and hydrazine vapor reduction. Nanoscale Research Letters, 2012, 7, 161. | 5.7 | 75 |
| 189 | In Situ Synthesis of Reduced Graphene Oxide and Gold Nanocomposites for Nanoelectronics and Biosensing. Nanoscale Research Letters, 2011, 6, 60. | 5.7 | 93 |
| 190 | Graphene-wrapped TiO2 hollow structures with enhanced lithium storage capabilities. Nanoscale, 2011, 3, 2158. | 5.6 | 223 |
| 191 | Assembly of Graphene Oxide and Au0.7Ag0.3 Alloy Nanoparticles on SiO2: A New Raman Substrate with Ultrahigh Signal-to-Background Ratio. Journal of Physical Chemistry C, 2011, 115, 24080-24084. | 3.1 | 36 |
| 192 | Fabrication and Characterization of Networked Graphene Devices Based on Ultralarge Single-Layer Graphene Sheets. IEEE Nanotechnology Magazine, 2011, 10, 467-471. | 2.0 | 4 |
| 193 | Micro- and Nanotechnologies for Study of Cell Secretion. Analytical Chemistry, 2011, 83, 4393-4406. | 6.5 | 72 |
| 194 | Mobility Enhancement in Carbon Nanotube Transistors by Screening Charge Impurity with Silica Nanoparticles. Journal of Physical Chemistry C, 2011, 115, 6975-6979. | 3.1 | 15 |
| 195 | Ultra-sensitive and wide-dynamic-range sensors based on dense arrays of carbon nanotube tips. Nanoscale, 2011, 3, 4854. | 5.6 | 34 |
| 196 | Electrical Detection of Metal Ions Using Field-Effect Transistors Based on Micropatterned Reduced Graphene Oxide Films. ACS Nano, 2011, 5, 1990-1994. | 14.6 | 279 |
| 197 | Quantum Dots with Phenylboronic Acid Tags for Specific Labeling of Sialic Acids on Living Cells. Analytical Chemistry, 2011, 83, 1124-1130. | 6.5 | 128 |
| 198 | The crosstalks between adipokines and catecholamines. Molecular and Cellular Endocrinology, 2011, 332, 261-270. | 3.2 | 21 |

| # | Article | IF | CITATIONS |
|-----|---|------|-----------|
| 199 | Transparent, Flexible, All-Reduced Graphene Oxide Thin Film Transistors. ACS Nano, 2011, 5, 5038-5044. | 14.6 | 305 |
| 200 | Graphene-based biosensors for detection of bacteria and their metabolic activities. Journal of Materials Chemistry, 2011, 21, 12358. | 6.7 | 343 |
| 201 | The formation of a carbon nanotube–graphene oxide core–shell structure and its possible applications. Carbon, 2011, 49, 5071-5078. | 10.3 | 130 |
| 202 | A graphene nanoribbon network and its biosensing application. Nanoscale, 2011, 3, 5156. | 5.6 | 81 |
| 203 | Nanoelectronic detection of triggered secretion of pro-inflammatory cytokines using CMOS compatible silicon nanowires. Biosensors and Bioelectronics, 2011, 26, 2746-2750. | 10.1 | 52 |
| 204 | Label-free, electrochemical detection of methicillin-resistant staphylococcus aureus DNA with reduced graphene oxide-modified electrodes. Biosensors and Bioelectronics, 2011, 26, 3881-3886. | 10.1 | 191 |
| 205 | Labeling and Tracking P2 Purinergic Receptors in Living Cells Using ATP onjugated Quantum Dots. Advanced Functional Materials, 2011, 21, 2776-2780. | 14.9 | 11 |
| 206 | Detecting metabolic activities of bacteria using a simple carbon nanotube device for high-throughput screening of anti-bacterial drugs. Biosensors and Bioelectronics, 2011, 26, 4257-4261. | 10.1 | 23 |
| 207 | Growth of large-sized graphene thin-films by liquid precursor-based chemical vapor deposition under atmospheric pressure. Carbon, 2011, 49, 3672-3678. | 10.3 | 158 |
| 208 | One-step growth of graphene–carbon nanotube hybrid materials by chemical vapor deposition. Carbon, 2011, 49, 2944-2949. | 10.3 | 182 |
| 209 | Differential effects of lysophospholipids on exocytosis in rat PC12 cells. Journal of Neural Transmission, 2010, 117, 301-308. | 2.8 | 19 |
| 210 | Changes in Brain Cholesterol Metabolome After Excitotoxicity. Molecular Neurobiology, 2010, 41, 299-313. | 4.0 | 54 |
| 211 | Electrical Detection of DNA Hybridization with Singleâ€Base Specificity Using Transistors Based on CVDâ€Grown Graphene Sheets. Advanced Materials, 2010, 22, 1649-1653. | 21.0 | 516 |
| 212 | Nanoelectronic Biosensing of Dynamic Cellular Activities Based on Nanostructured Materials. Advanced Materials, 2010, 22, 2818-2823. | 21.0 | 42 |
| 213 | Nonâ€invasive Detection of Cellular Bioelectricity Based on Carbon Nanotube Devices for Highâ€Throughput Drug Screening. Advanced Materials, 2010, 22, 3199-3203. | 21.0 | 26 |
| 214 | Sugarâ€Based Synthesis of Tamiflu and Its Inhibitory Effects on Cell Secretion. Chemistry - A European Journal, 2010, 16, 4533-4540. | 3.3 | 48 |
| 215 | Integrating carbon nanotubes and lipid bilayer for biosensing. Biosensors and Bioelectronics, 2010, 25, 1834-1837. | 10.1 | 46 |
| 216 | Vesicular storage, vesicle trafficking, and secretion of leptin and resistin: the similarities, differences, and interplays. Journal of Endocrinology, 2010, 206, 27-36. | 2.6 | 38 |

| # | Article | IF | CITATIONS |
|-----|---|------------------------------|-----------|
| 217 | Aromatic Molecules Doping in Single-Layer Graphene Probed by Raman Spectroscopy and Electrostatic Force Microscopy. Japanese Journal of Applied Physics, 2010, 49, 01AH04. | 1.5 | 10 |
| 218 | Bidirectional mediation of TiO2 nanowires field effect transistor by dipole moment from purple membrane. Nanoscale, 2010, 2, 1474. | 5.6 | 15 |
| 219 | Carbohydrate functionalized carbon nanotubes and their applications. Chemical Society Reviews, 2010, 39, 2925. | 38.1 | 87 |
| 220 | Ultra-large single-layer graphene obtained from solution chemical reduction and its electrical properties. Physical Chemistry Chemical Physics, 2010, 12, 2164. | 2.8 | 176 |
| 221 | Effects of cholesterol oxidation products on exocytosis. Neuroscience Letters, 2010, 476, 36-41. | 2.1 | 32 |
| 222 | Centimeter-Long and Large-Scale Micropatterns of Reduced Graphene Oxide Films: Fabrication and Sensing Applications. ACS Nano, 2010, 4, 3201-3208. | 14.6 | 571 |
| 223 | Nanoelectronic biosensors based on CVD grown graphene. Nanoscale, 2010, 2, 1485. | 5.6 | 408 |
| 224 | Interfacing Live Cells with Nanocarbon Substrates. Langmuir, 2010, 26, 2244-2247. | 3.5 | 301 |
| 225 | Surface immobilized cholera toxin B subunit (CTB) facilitates vesicle docking, trafficking and exocytosis. Integrative Biology (United Kingdom), 2010, 2, 250. | 1.3 | 12 |
| 226 | CMOS ompatible Nanowire Sensor Arrays for Detection of Cellular Bioelectricity. Small, 2009, 5, 208-212. | 10.0 | 98 |
| 227 | Effective doping of single-layer graphene from underlying <mml:math xmlns:mml="http://www.w3.org/1998/Math/MathML" display="inline"><mml:mrow><mml:msub><mml:mrow><mml:mtext>SiO</mml:mtext></mml:mrow><mml:mn> Physical Review B, 2009, 79, .</mml:mn></mml:msub></mml:mrow></mml:math | 2< 3;2 2 <b imml:m | n> |
| 228 | Nanotopographic Carbon Nanotube Thinâ€Film Substrate Freezes Lateral Motion of Secretory Vesicles. Advanced Materials, 2009, 21, 790-793. | 21.0 | 24 |
| 229 | Interfacing Glycosylated Carbonâ€Nanotubeâ€Network Devices with Living Cells to Detect Dynamic Secretion of Biomolecules. Angewandte Chemie - International Edition, 2009, 48, 2723-2726. | 13.8 | 148 |
| 230 | PKC epsilon facilitates recovery of exocytosis after an exhausting stimulation. Pflugers Archiv European Journal of Physiology, 2009, 458, 1137-1149. | 2.8 | 10 |
| 231 | Label-free detection of ATP release from living astrocytes with high temporal resolution using carbon nanotube network. Biosensors and Bioelectronics, 2009, 24, 2716-2720. | 10.1 | 62 |
| 232 | Doping Single‣ayer Graphene with Aromatic Molecules. Small, 2009, 5, 1422-1426. | 10.0 | 537 |
| 233 | Using oxidation to increase the electrical conductivity of carbon nanotube electrodes. Carbon, 2009, 47, 1867-1870. | 10.3 | 152 |
| 234 | Involvement of PKCα in PMA-induced facilitation of exocytosis and vesicle fusion in PC12 cells. Biochemical and Biophysical Research Communications, 2009, 380, 371-376. | 2.1 | 21 |

| # | Article | IF | CITATIONS |
|-----|---|------|-----------|
| 235 | Roles of Cholesterol in Vesicle Fusion and Motion. Biophysical Journal, 2009, 97, 1371-1380. | 0.5 | 91 |
| 236 | Ultra-sensitive detection of adipocytokines with CMOS-compatible silicon nanowire arrays. Nanoscale, 2009, 1, 159. | 5.6 | 54 |
| 237 | Symmetry Breaking of Graphene Monolayers by Molecular Decoration. Physical Review Letters, 2009, 102, 135501. | 7.8 | 224 |
| 238 | In Situ Synthesis of Metal Nanoparticles on Single-Layer Graphene Oxide and Reduced Graphene Oxide Surfaces. Journal of Physical Chemistry C, 2009, 113, 10842-10846. | 3.1 | 702 |
| 239 | One-Pot Synthesis of Carbon-Coated SnO ₂ Nanocolloids with Improved Reversible Lithium Storage Properties. Chemistry of Materials, 2009, 21, 2868-2874. | 6.7 | 421 |
| 240 | Solution-processable semiconducting thin-film transistors using single-walled carbon nanotubes chemically modified by organic radical initiators. Chemical Communications, 2009, , 7182. | 4.1 | 33 |
| 241 | Effects of phorbol ester on vesicle dynamics as revealed by total internal reflection fluorescence microscopy. Pflugers Archiv European Journal of Physiology, 2008, 457, 211-222. | 2.8 | 17 |
| 242 | Label-Free Electronic Detection of DNA Using Simple Double-Walled Carbon Nanotube Resistors. Journal of Physical Chemistry C, 2008, 112, 9891-9895. | 3.1 | 37 |
| 243 | Detecting translocation of individual single stranded DNA homopolymers through a fabricated nanopore chip. Frontiers in Bioscience - Landmark, 2007, 12, 2978. | 3.0 | 10 |
| 244 | Nanopore Unstacking of Single-Stranded DNA Helices. Small, 2007, 3, 1204-1208. | 10.0 | 22 |
| 245 | Comparison of biochemical effects of statins and fish oil in brain: The battle of the titans. Brain Research Reviews, 2007, 56, 443-471. | 9.0 | 97 |
| 246 | Differential effects of ceramide species on exocytosis in rat PC12 cells. Experimental Brain Research, 2007, 183, 241-247. | 1.5 | 25 |
| 247 | Probing Single DNA Molecule Transport Using Fabricated Nanopores. Nano Letters, 2004, 4, 2293-2298. | 9.1 | 341 |
| 248 | Atomic Layer Deposition to Fine-Tune the Surface Properties and Diameters of Fabricated Nanopores. Nano Letters, 2004, 4, 1333-1337. | 9.1 | 385 |
| 249 | Amperometric Detection of Quantal Catecholamine Secretion from Individual Cells on Micromachined Silicon Chips. Analytical Chemistry, 2003, 75, 518-524. | 6.5 | 86 |
| 250 | A highly Ca2+-sensitive pool of vesicles is regulated by protein kinase C in adrenal chromaffin cells. Proceedings of the National Academy of Sciences of the United States of America, 2002, 99, 17060-17065. | 7.1 | 83 |
| 251 | The Relationship between Camp, Ca2+, and Transport of Cftr to the Plasma Membrane. Journal of General Physiology, 2001, 118, 135-144. | 1.9 | 28 |
| 252 | The Noise of Membrane Capacitance Measurements in the Whole-Cell Recording Configuration. Biophysical Journal, 2000, 79, 2162-2170. | 0.5 | 46 |

| # | Article | IF | CITATIONS |
|-----|--|-----|-----------|
| 253 | A novel microfabricated device measures a large fraction of hormone release from individual-cells with high time resolution. , 0, , . | | 0 |
| 254 | Nanopore Devices for Single Molecule Sensing. , 0, , . | | 0 |
| 255 | Facile Synthesis of TiO ₂ Microspheres with Super High Rate Performance. Advanced Materials Research, 0, 573-574, 1198-1202. | 0.3 | 0 |